Solution processable organic/inorganic hybrid ultraviolet photovoltaic detector

Xiaopeng Guo [iD], Libin Tang, Jinzhong Xiang, Rongbin Ji, Kai Zhang, Sin Ki Lai, Jun Zhao, Jincheng Kong, and Shu Ping Lau
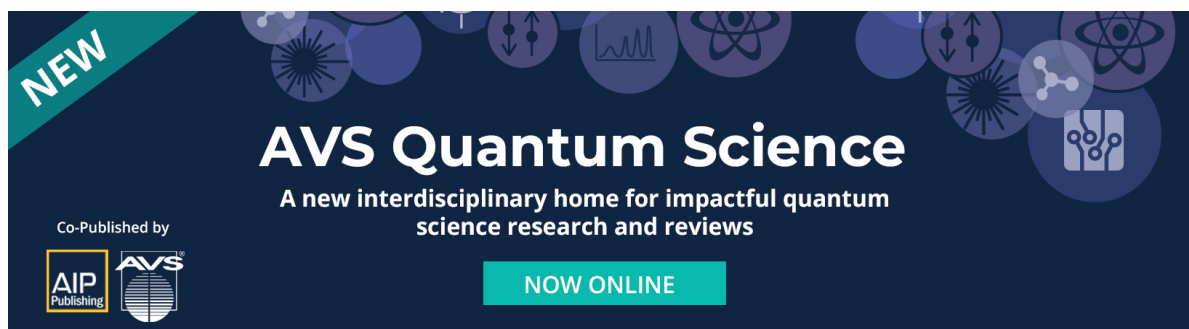
View Online   Export Citation   CrossMark

ARTICLES YOU MAY BE INTERESTED IN

High performance ultraviolet photodetectors based on ZnO nanoflakes/PVK heterojunction
Applied Physics Letters **109**, 073103 (2016); https://doi.org/10.1063/1.4961114

Large-area uniform electron doping of graphene by Ag nanofilm
AIP Advances **7**, 045209 (2017); https://doi.org/10.1063/1.4979113

ZnO/poly(9,9-dihexylfluorene) based inorganic/organic hybrid ultraviolet photodetector
Applied Physics Letters **93**, 153309 (2008); https://doi.org/10.1063/1.3003881

Solution processable organic/inorganic hybrid ultraviolet photovoltaic detector

Xiaopeng Guo,[1] Libin Tang,[2,a] Jinzhong Xiang,[1,b] Rongbin Ji,[2,c] Kai Zhang,[3] Sin Ki Lai,[4] Jun Zhao,[2] Jincheng Kong,[2] and Shu Ping Lau[4]

[1]*School of Materials Science and Engineering, Yunnan University, Kunming 650091, P.R.China*
[2]*Kunming Institute of Physics, Kunming 650223, P.R.China*
[3]*Suzhou Institute of Nano-Tech and Nano-Bionics(SINANO), Chinese Academy of Sciences, Suzhou 215123, P.R.China*
[4]*Department of Applied Physics, The Hong Kong Polytechnic University, Hong Kong SAP, P.R.China*

Ultraviolet (UV) photodetector is a kind of important optoelectronic device which can be widely used in scientific and engineering fields including astronomical research, environmental monitoring, forest-fire prevention, medical analysis, and missile approach warning *etc*. The development of UV detector is hindered by the acquirement of stable *p*-type materials, which makes it difficult to realize large array, low-power consumption UV focal plane array (FPA) detector. Here, we provide a novel structure (Al/Poly(9,9-di-n-octylfuorenyl-2,7-diyl)(PFO)/ZnO/ITO) to demonstrate the UV photovoltaic (PV) response. A rather smooth surface (RMS roughness: 0.28 nm) may be reached by solution process, which sheds light on the development of large-array, light-weight and low-cost UV FPA detectors. © *2016 Author(s). All article content, except where otherwise noted, is licensed under a Creative Commons Attribution (CC BY) license (http://creativecommons.org/licenses/by/4.0/).* [http://dx.doi.org/10.1063/1.4952425]

I. INTRODUCTION

Ultraviolet (UV) photodetector has been receiving increasingly attention due to its important applications in civilian and military fields including astronomical research, environmental monitoring, forest-fire prevention, medical analysis, and missile approach warning *etc*. The development of UV photodetector is working towards large-array, high-performance, fast-response, light-weight and low-cost products. Up to now a lot of materials have been used as UV sensitive materials, including Si,[1] SiC,[2] diamond,[3] TiO$_2$,[4] GaN,[5] ZnO,[6] *etc*. However, the development of UV focal plane array is hindered by the acquirement of stable *p*-type materials. Recently, the presence of organic UV semiconductor provides a feasible solution.

Organic/inorganic heterojunction may take advantage of both inorganic and organic semiconductors, providing more free degrees in device design. Nowadays, a number of organic UV semiconductors have been explored as UV sensitive materials, including 2,9-dimethyl-4,7-diphenyl-1,10-phenanthroline (BCP),[7] Phenanthrene,[8] and PFO[9] *etc*. Among them PFO is a polymer that can be processed by solution method. Recently, Yun-Yue Lin *et al*.[10] have fabricated a near-UV photodetector utilizing the hybrid of PFO and *n*-ZnO nanorods, with the structure of ITO glass/*n*-ZnO nanorods/PFO/PEDOT:PSS/Au. They integrated ZnO with PFO successfully and manufactured a well performed near-UV device, but some new drawbacks were introduced at the same time. The ZnO nanorods with rough surface is hard to be used in the large array device, because the PEDOT:

---

[a]E-mail: scitang@163.com
[b]E-mail: jzhxiang@ynu.edu.cn
[c]E-mail: jirongbin@gmail.com

PSS transport layer is not easy to coat over the ZnO nanorods, which unavoidably makes the fabrication more complex, and difficult to scale-up.

Here, we provide a novel structure (Al/PFO/ZnO/ITO) to demonstrate the UV photovoltaic (PV) response, the key hybrid heterojunction was fabricated by solution process, importantly, a rather smooth surface (RMS roughness: 0.28 nm) is reached, showing important potential applications in large-array, light-weight, low-cost UV FPA detectors.

II. EXPERIMENTAL

A. Detailed chemicals information

H_2O_2 (30% AR), $NH_3 \cdot H_2O$ (26%-30% AR), ethanolamine (99%-100% AR) were purchased from Tianjin Fengchuan Chemical Reagent Co., Ltd. (Tianjin, China). Zinc acetate dihydrate (99.0% AR) was purchased from Bodi Chemical Co., Ltd. (Tianjin, China). Ethanol (99.8% AR), ethylene glycol (AR) and glacial acetic acid (99.5% AR) were purchased from Chengdu Kelong Chemical Co., Ltd. (Sichuan, China). All the chemicals were used without further purification.

B. Fabrication

The fabrication process of the PFO/ZnO hybrid UV photodetector is shown in Figure 1(a). ZnO sol-gel (1 g zinc acetate dihydrate dissolved in a mixture solvent of 30 mL ethanol, 0.5 mL ethanolamine, 1 mL ethylene glycol and 0.5 mL glacial acetic acid) was firstly dropped onto ITO glass (MTI, 30 Ωsq^{-1}), after spin-coating (3800 rpm, 60 s) and heating (400 °C, 2 hr), ZnO film was prepared on ITO glass. 40 mg mL^{-1} PFO (Xi'an *p*-OLED) solution (CHCl$_3$ as solvent) was spin-coated (1500 rpm, 30 s) on ZnO film to form PFO/ZnO heterojunction. Then, the top electrode was coated by thermal evaporating Al on the surface of PFO. Finally, Au wire was bonded with Al and ITO to complete device fabrication.
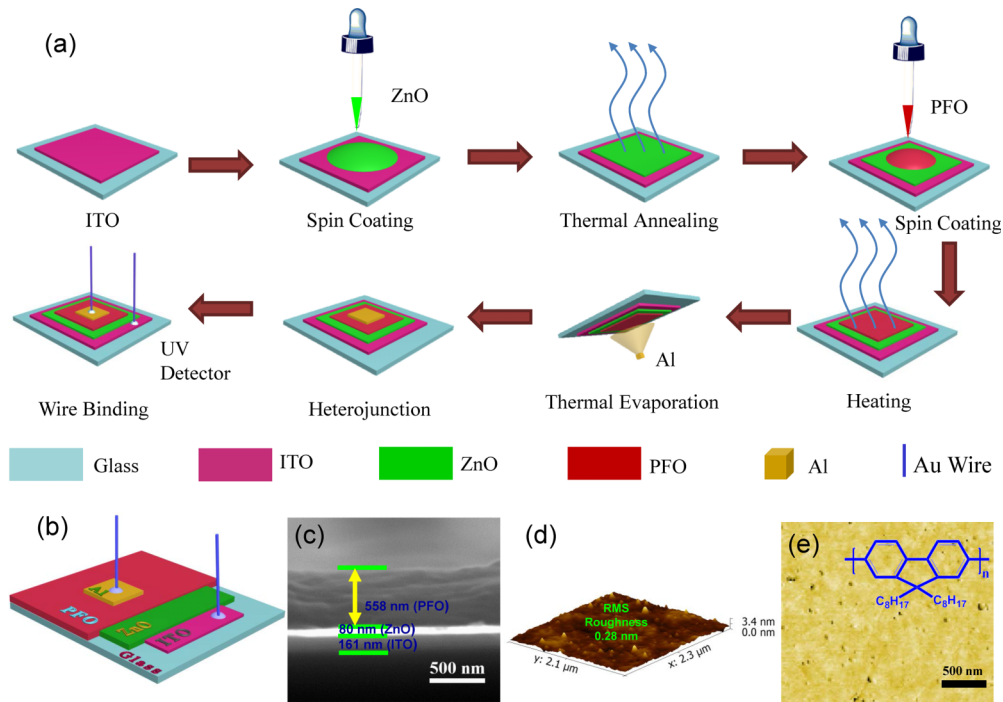

FIG. 1. (a) The schematic illustration for fabrication of PFO/ZnO hybrid UV detector. (b) The schematic diagram of the PFO/ZnO hybrid UV detector. (c) The cross-sectional SEM image of the device. (d) The AFM image of PFO film. (e) The phase image of PFO film, inset: the molecular structure of PFO.

C. Characterization

The cross-sectional view of the device was investigated by scanning electron microscope (SEM) (Hitachi S3400, Japan) (30.0kV). The surface morphology and roughness were studied by atomic force microscope (AFM) (SPA-400). UV-Vis absorption spectra were measured using a Horiba iHR-320 spectrometer. The Raman spectra were obtained by Renishaw in Via Raman microscope with a wavelength of 514.5 nm. The X-ray diffraction (XRD) patterns of the samples were measured by Rigaku D/Max-23 at room temperature. The photoluminescence (PL) and PL excitation (PLE) spectra were measured using photoluminescence spectrometer (Hitachi F-4500 and F-7000). The ellipsometric spectra were measured using JY Auto SE instrument. The current density-voltage (*J-V*) characteristics were tested with a Keithley 2400 source meter.

III. RESULTS AND DISCUSSION

The schematic diagram of the device is shown in Figure 1(b). The layer thickness was investigated by scanning electron microscope (SEM). Figure 1(c) shows the cross-sectional view of the device revealing the thicknesses of ITO, ZnO and PFO films are 161, 80 and 558 nm, respectively. Roughness plays an important role in device performance, Figures 1(d) and 1(e) indicate that the spin-coated PFO film shows an uniform and smooth surface (RMS roughness: 0.28 nm), which meets the requirements for a high performance.

Structural and optical properties play key roles in affecting device performance. The PFO/ZnO heterojunction may broaden the absorption band as shown in Figure 2(a). The FWHMs of absorption peak for ZnO and PFO films are 42.0 and 67.5 nm respectively, their heterojunction gives 69.5 nm. This important result may be due to the following fact: both junction components (ZnO and PFO films) can absorb UV photons efficiently, and the photogenerated electrons (holes) flow to ZnO (PFO) because of the electric potential difference between the two layers (as shown in the inset of Figure 2(a)). The XRD pattern of the heterojunction (Figure 2(b)) shows that ZnO takes on crystalline structure (Figure 3(a)), while PFO shows no distinct diffraction peaks probably due to its
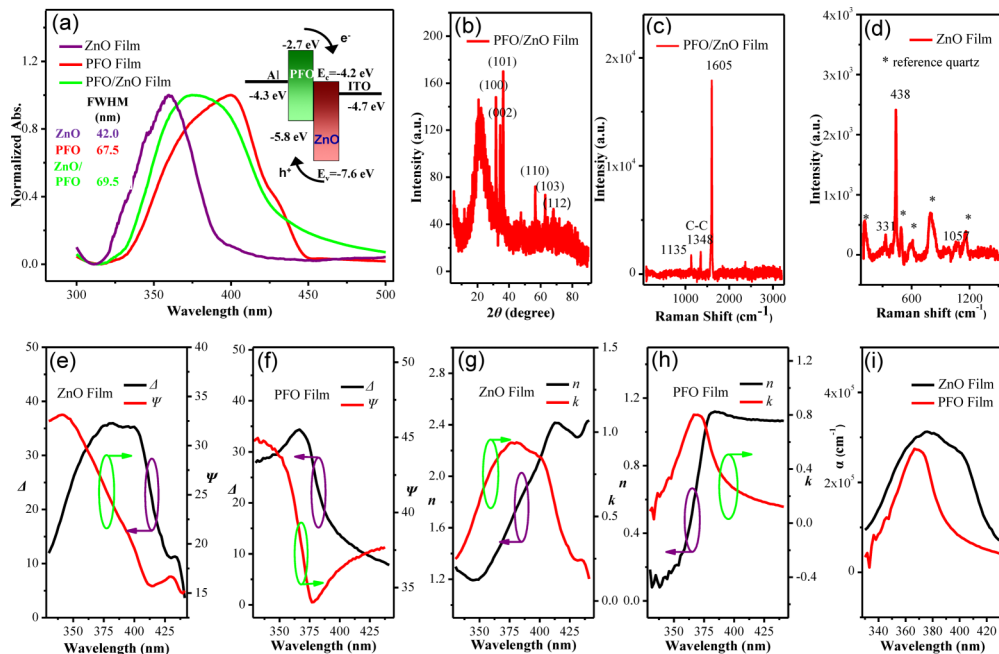

FIG. 2. (a) The normalized UV-Vis absorption spectra for ZnO, PFO, and PFO/ZnO films. The XRD pattern (b) and Raman spectrum (c) of PFO/ZnO film. (d) The Raman spectrum of ZnO film. (e) and (g) The optical parameters for ZnO film measured by spectroscopic ellipsometry. (f) and (h) The optical parameters for PFO film measured by spectroscopic ellipsometry. (i) The absorption coefficients for ZnO and PFO films.
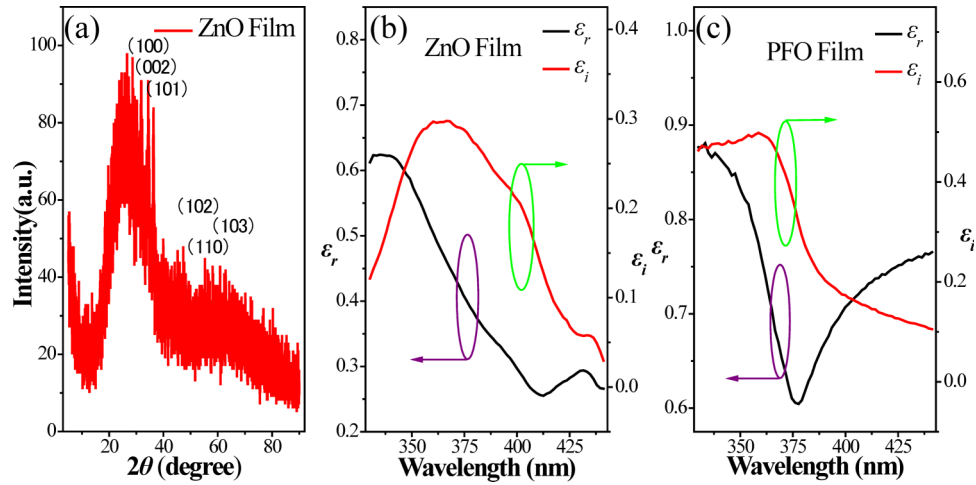
FIG. 3. (a) The XRD pattern of ZnO film. (b), (c) The dielectric parameters of ZnO and PFO films measured by spectroscopic ellipsometry.

amorphous structure. The Raman investigation (Figure 2(c)) on the heterojunciton shows obvious vibration peaks (C-C: 1135 and 1348 cm^{-1}; C=C: 1605 cm^{-1}) caused by PFO,[11] no apparent ZnO Raman peaks have been observed in the heterojunction because of the underneath weak ZnO signal has been blocked by top layer of PFO. The sole ZnO crystalline film presents characteristic Raman peaks[12] at 331, 438 and 1057 cm^{-1} as shown in Figure 2(d).

The optical properties of the active layers were studied by spectroscopic ellipsometry (SE). The important wavelength dependent optical parameters such as reflective index (n) and extinction coefficient (k) may be calculated from the measured amplitude (Ψ) and phase (Δ) data through the Kramers-Kronig relation, Figures 2(e)-2(f) and Figures 3(b)-3(c) are the SE results, based on these data, the absorption coefficients (α) for ZnO and PFO films may be derived. Importantly, both ZnO and PFO films show a very large absorption coefficient ($\alpha > 2 \times 10^5$ cm^{-1}) at ~ 370 nm, meaning that a very thin film in the heterojunction could meet the sufficient UV absorption requirements, which is important for developing light-weight, fast-response, solid-state UV photodetector.

The photoluminescence (PL) and PL excitation (PLE) spectra for ZnO, PFO and their hybrid films were studied. The results are shown in Figure 4. ZnO film shows a strong PL emission peak at ~ 400 nm excited by various λ_{ex} ranging from 280 to 360 nm with a step of 20 nm (Figure 4(a)). The PLE spectra measured at different receiving energies (λ_{em}) show a single strong peak in UV range (Figure 4(d)), which corresponds well with UV-Vis absorption result. Figure 4(b) shows that PFO has multiple PL peaks in the range of 400-550 nm, the multiple peaks are resulted from the electron transitions (in various vibration states) from excited state (S1) to ground state (S0). The PLE spectra (Figure 4(e)) show that PFO has a strong peak in 300-440 nm. For the hybrid film (PFO/ZnO), both PL and PLE spectra (Figure 4(c), 4(f)) show different shapes compared with sole ZnO and sole PFO films, meaning that the interaction between PFO and ZnO layers.

The device performance is shown in Figure 5. As shown in Figures 5(a) and 5(b), the PFO/ZnO hybrid UV detector has the rectification effects both in the dark and with UV illumination, a stronger illumination results in a bigger current density (J), indicating the device has the UV response. Figure 5(c) shows the bias voltage dependent responsivity (R) curves, it can be seen that a larger bias voltage leads to a bigger R, a value bigger than 40 mA W^{-1} is gotten at 2 V bias under a power density of 0.01 mW cm^{-2}. Detectivity (D^*) is an important parameter to evaluate a photodetector, D^* can be calculated as,[13]

$$D^* = R/\sqrt{2qJ_d} \tag{1}$$

where q and J_d are the absolute electron charge and the dark current density, respectively. The voltage dependent D^* curves are shown in Figure 5(d). Clearly, D^* increases with bias voltage. UV power density also affects D^*, for a fixed bias voltage, D^* increases with decreasing power density.
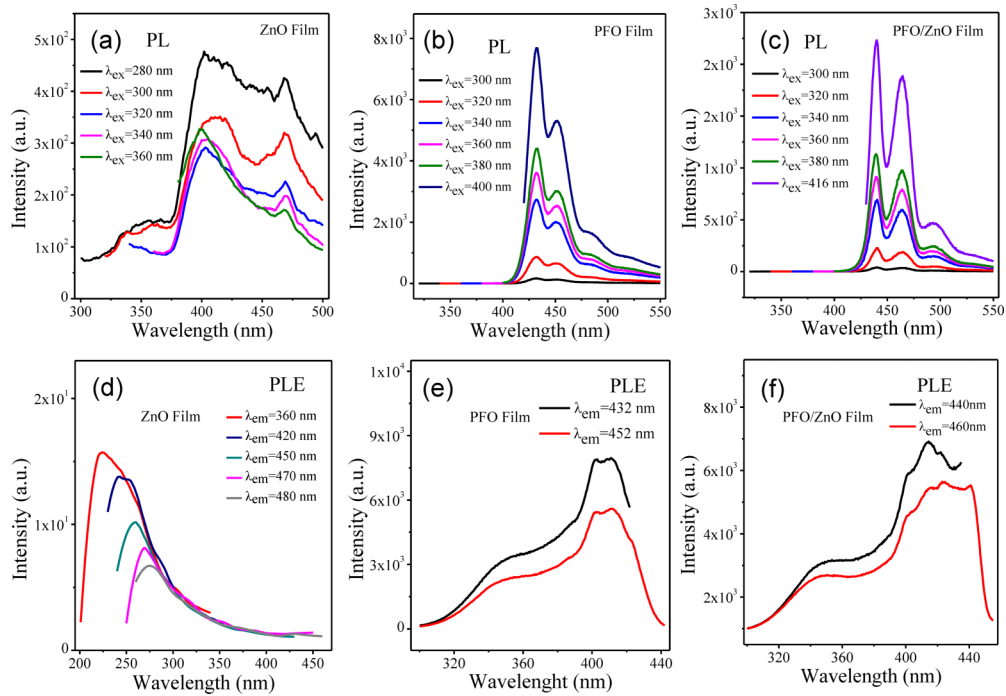
FIG. 4. The PL and PLE spectra for ZnO film, PFO film and their hybrid. (a), (b), (c) are PL spectra for ZnO, PFO and PFO/ZnO films, respectively. (d), (e), (f) are PLE spectra for ZnO, PFO and PFO/ZnO films, respectively.

A value $> 3 \times 10^{10}$ cmHz$^{1/2}$ W^{-1} has been reached at a bias voltage of 2 V (under 0.01 mW cm^{-2}) for the un-optimized device, This value is comparable to that of inorganic GaN, ZnO,TiO$_2$ photodetectors and other previously reported organic or inorganic UV photodetectors as shown in the supplementary material.[14]
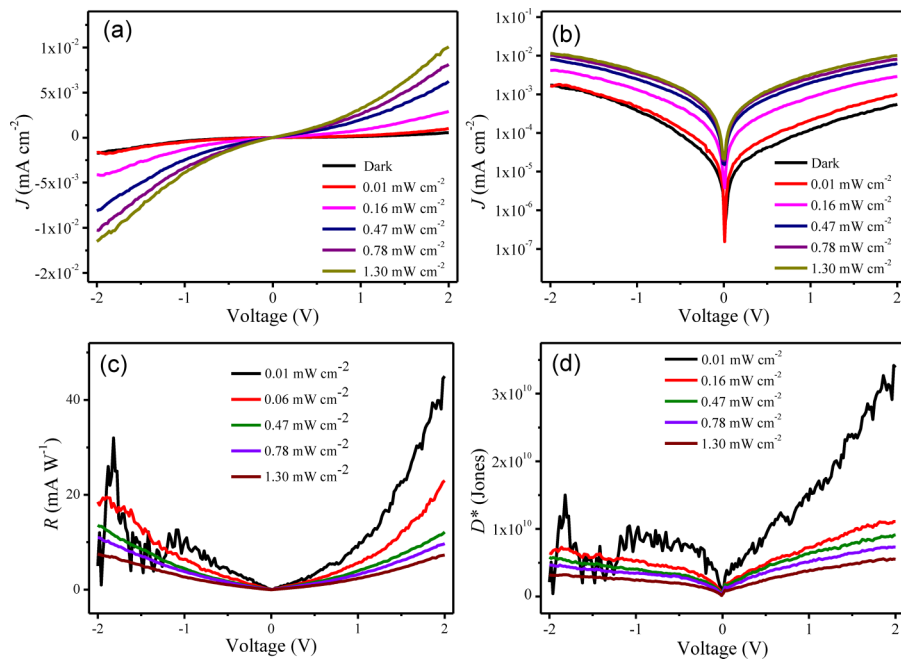

FIG. 5. The device performance of PFO/ZnO hybrid UV detector. (a)*J*-*V* curves, (b) log(*J*)-*V* curves, (c) *R* (Responsivity)-*V* curves, (d) *D** (Detectivity)-*V* curves.

TABLE I. The ideality factors (n), reverse saturation current densities (J_0) and barrier heights (Φ_b) of the device under different power intensities.

Power Density (mW cm^{-2})	n	J_0 (mA cm^{-2})	Φ_b (eV)
Dark	0.78	1.98×10^{-7}	0.76
0.01	0.43	8.17×10^{-8}	0.78
0.16	0.56	1.86×10^{-6}	0.70
0.47	1.02	1.12×10^{-5}	0.66
0.78	1.00	1.43×10^{-5}	0.65
1.30	0.99	1.56×10^{-5}	0.65

To understand the underlying physical mechanism of the device, the electrical parameters of the device has been studied more deeply. The J-V characteristics of the device is given by eqn. (2), which is based on the thermionic emission theory,[15]

$$J = J_0 \left[\exp\left(\frac{qV}{nk_BT} \right) - 1 \right] \qquad (2)$$

where J_0 is the reverse saturation current density, q unit charge, n the ideality factor, k_B the Boltzman constant, and T the absolute temperature. For equ. (2), since $qV \gg nk_BT$, thus $\ln(J) = \ln J_0 + \frac{qV}{nk_BT}$, $n = \left(\frac{d\ln J}{dV} \frac{k_BT}{q} \right)^{-1}$, therefore, the ideality factor n can be calculated from the slope of $\ln J$-V curve.[16]

Barrier heights Φ_b can be calculated using the Richardson equation,

$$J_0 = A^*T^2 \exp\left(-\frac{q\Phi_b}{k_BT} \right) \qquad (3)$$

where $A^* = \frac{4\pi q m^* k_B^2}{h^3}$[17] is the effective Richardson constant, m^* is the effective electron mass, which is achieved according to the equation:

$$m^* = m^*(\text{ZnO})50\% + m^*(\text{PFO})50\% \qquad (4)$$

where $m^*(\text{ZnO}) = 0.24$,[18] and $m^*(\text{PFO}) \approx 0.394$.

The ideality factors (n), reverse saturation current densities (J_0) and barrier heights (Φ_b) of the device under different power intensities have been calculated and listed in Table I.

Ideality factor (n) is an important parameter to evaluate the electrical behavior of the diode, it is also called as the curve shape factor, which indicates a deviation from the ideal value. Many factors such as interfacial layers, barrier inhomogeneity, image force lowering, series resistance, $etc.$ may cause a dramatic deterioration of electrical properties of the diodes.[19] When a diode has an ideality factor close to 1, it can be viewed as an ideal diode, in which charge carrier tends to diffuse.[20] The ideality factors (n) listed in Table I are close to 1, meaning that the device shows good rectification property, which plays an important role in high-performance photodetector.

IV. CONCLUSION

An organic/inorganic hybrid UV photovoltaic detector has been developed by using PFO/ZnO heterojunction. The device structure (Al/PFO/ZnO/ITO) may reach a rather smooth surface (RMS roughness: 0.28nm) which is a key parameter for large-array, high-uniformity UV FPA detectors. The PFO/ZnO heterojunction may broaden the absorption band, absorbing more UV photons that is important for high-sensitive device. The un-optimized device shows a $D^* > 3 \times 10^{10}$ cmHz$^{1/2}$ W^{-1} at 2 V bias voltage under 0.01 mW cm^{-2} at room temperature. The study paves the way for developing large-array, high-performance, high-uniformity, light-weight and low-cost UV FPA detectors which have important applications in astronomical research, environmental monitoring, forest-fire prevention, medical analysis, and missile approach warning.

ACKNOWLEDGMENTS

[1] I. Khodami, F. Taghibakhsh, and K. S. Karim, IEEE Electron Device Lett. **29**, 1007 (2008).
[2] A. Sciuto, F. Roccaforte, and V. Raineri, Appl. Phys. Lett. **92**, 093505 (2008).
[3] A. Balducci, M. Marinelli, E. Milani, M. E. Morgada, A. Tucciarone, and G. Verona-Rinati, Appl. Phys. Lett. **86**, 19350 (2005).
[4] S. Sharma, A. R. Pal, J. Chutia, H. Bailung, N. S. Sarma, N. N. Dass, and D. Patil, Appl. Surf. Sci. **258**, 7897 (2012).
[5] B. P. Rafael and G. C. Manuel, Mater. Lett. **159**, 110 (2015).
[6] M. H. Huang, S. Mao, H. Feick, H. Q. Yan, Y. Y. Wu, H. Kind, E. Weber, R. Russo, and P. D. Yang, Science **292**, 1897 (2001).
[7] Y. H. Cai, L. B. Tang, J. Z. Xiang, R. B. Ji, J. Zhao, J. Yuan, Y. Duan, Y. B. Hu, Y. J. Tai, and J. H. Zhao, J. Appl. Phys. **118**, 124503 (2015).
[8] W. T. Cheng, L. B. Tang, J. Z. Xiang, R. B. Ji, and J. Zhao, RSC Adv. **6**, 12076 (2016).
[9] X. F. Xu, B. Han, J. W. Chen, J. B. Peng, H. B. Wu, and Y. Cao, Macromolecules **44**, 4204 (2011).
[10] Y. Y. Lin, C. W. Chen, W. C. Yen, W. F. Su, C. H. Ku, and J. J. Wu, Appl. Phys. Lett. **92**, 233301 (2008).
[11] P. Lukaszczuk, E. Borowiak-Palen, M. H. Rümmeli, and R. J. Kalenczuk, Phys. Status Solidi B **246**, 2699 (2009).
[12] R. C. Lima, L. R. Macario, J. W. M. Espinosa, V. M. Longo, R. Erlo, N. L. Marana, J. R. Sambrano, M. L. dos Santos, A. P. Moura, P. S. Pizani, J. Andrés, E. Longo, and J. A. Varela, J. Phys. Chem. A **112**, 8970 (2008).
[13] X. Gong, M. H. Tong, Y. J. Xia, W. Z. Cai, J. S. Moon, Y. Cao, G. Yu, C. L. Shieh, B. Nilsson, and A. J. Heeger, Science **365**, 1665 (2009).
[14] See supplementary material at http://dx.doi.org/10.1063/1.4952425 for the comparison of the PFO/ZnO hybrid UV detector fabricated in this paper with some common UV detectors (supplementary Table S1).
[15] S. Tongay, M. Lemaitre, X. Miao, B. Gila, B. R. Appleton, and A. F. Hebard, Phys. Rev. X **2**, 011002 (2012).
[16] G. A. H. Wetzelaer and P. W. M. Blom, NPG Asia Mater. **6**, e110 (2014).
[17] J. H. Zhao, L. B Tang, J. Z. Xiang, R. B. Ji, Y. B. Hu, J. Yuan, J. Zhao, Y. J. Tai, and Y. H. Cai, RSC Adv. **5**, 29222 (2015).
[18] M. Oshikiri, Y. Imanaka, F. Aryasetiawan, and G. Kido, Phys. B **298**, 472 (2001).
[19] B. Gunduz, I. S. Yahia, and F. Yakuphanoglu, Microelectron. Eng. **98**, 41 (2012).
[20] P. N. Uppal, G. Charache, P. Baldasaro, B. Campbell, S. Loughin, S. Svensson, and D. Gill, J Cryst Growth **175**, 877 (1997).